Modeling rotating fiber jets and application in forcespinning

Dr. Daniel N. Riahi

School of Mathematical & Statistical Sciences, University of Texas Rio Grande Valley, Brownsville Campus
(E-mail:daniel.riahi@utrgv.edu)

Abstract: In this lecture we first review modeling and simulation that have been carried out in the last two decades for nonlinear inviscid and viscous Newtonian rotating jets with curved centerlines. Next, we explain our recently developed modeling equations for the non-Newtonian polymeric fiber jets and calculate numerically the corresponding nonlinear solutions for quantities such as jet speed, radius, stretching rate, trajectory and strain rate versus different values of the arc length and the parameters that can represent effects due to rotation, friction, surface tension and relaxation time. We present application of such results in forcespinning process, a relatively new technology that uses centrifugal force due to an externally imposed rotational constraint to produce nanofibers from different materials and with important technological applications. We also briefly describe on our more recent results for non-Newtonian jets.

1.Introductory materials

In the last several years there have been mostly experimental investigations in developing and using the forcespinning method (Dr. Lozano's Research Group: Padron et al. 2011, 2013; Vazquez et al. 2012; Altecor et al. 2012) which indicated possibility for prediction of nanofibers subjected to some trial-error based cases by FS procedure.

FS is a technology that uses centrifugal force due to an externally imposed rotational forces by a high rotational speed of a spinneret in a melt container to produce micro and nano fibers of polymer or other materials with important technological applications.

An important advantage of FS technique is in its high production rate as well as its applicability to different materials such as polymer, composite, metal, ceramic, etc. For example, its production rate per unit time is about over several hundred times more than the corresponding one by electrospinning process.

In the last decade or so there have been some theoretical and computational modeling of the dynamics of the liquid jets for Newtonian inviscid or viscous fluids (Decent et al. 2002; Wallwork et al. 2002; Parau et al. 2007; Decent et al. 2009; Padron et al. 2011; Padron et al. 2012; Taghavi

and Larson 2014a, b) due to the presence of centrifugal forces and based on the slender jet theory, where the aspect ratio for the fiber jet is assumed to be sufficiently small.

Decent et al. (2002) did modeling and computation for the dynamics of an inviscid liquid jet, which was emerged from a rotating drum. The authors investigated both linear temporal and linear spatial instability of steady basic state solution for the jet. For the linear temporal stability analysis, the authors found that axisymmetric mode can be unstable. Their linear spatial instability analysis also indicated instability of the jet.

Wallwork et al. (2002) investigated a slender inviscid liquid jet, which was due to a rotating orifice in the liquid zone. The authors used a model for inviscid jet in the presence of surface tension. They determined the trajectory of the jet, and they also calculated the linear jet instability. They found, in particular, that such basic state becomes unstable with respect to infinitesimal travelling wave modes that grow along the jet.

Parau et al. (2007) investigated the evolution of a disturbance on a rotating, slender jet. Using an asymptotic approach, they determined the equations for their modeling liquid jet. They determined, in particular, the steady solution for the liquid jet and found the effect of viscosity on the trajectory of the centerline and the radius of the jet. They also carried out

numerical simulation to examine the break-up of the liquid jet. Decent et al. (2009) studied the trajectory and linear stability of a liquid viscous jet using a Newtonian fluid. However, the leading order of their asymptotic model did not produce any effect of viscosity on their steady solution. But they found that by including the higher order terms in their model, then increasing Newtonian viscosity has the effect of making their jet solution less destabilized.

Padron et al. (2011) did modeling and computation of a two-dimensional FS for the inviscid rotating jet and in the presence of surface tension. They developed a two-dimensional inviscid modeling system from the governing Euler and Continuity equations and the associated boundary conditions for FS system. They solved numerically their modeling system and determined, in particular, fiber trajectory and the fiber radius versus arc length and for different values of the surface tension rotation effects. They found jet radius decreases with increasing rotation rate and increases with surface tension effect.

More recently Taghavi and Larson (2014a) investigated steady state problem for Newtonian jet flow formation by centrifugal spinning. They developed a so-called regularized thin-fiber modeling approach that made the steady state solution of the jet be affected by the presence of viscous

effect. Taghavi and Larson (2014b) corrected a number of errors that existed in their earlier paper (Taghavi and Larson 2014a) and included a revised version of several figures for the jet speed and trajectory.

All the theoretical and computational studies so far on the subject of rotating jets which were described above were for the Newtonian inviscid or viscous fluid flow cases. Here as a first step, we consider the polymeric fiber jet during FS process by making use of an empirical viscosity model for the polymeric non-Newtonian fluid. It is due to the variation of the elongational viscosity of the polymer fluid, which can create the so-called extension thinning and is possible to be represented by a variable viscosity as a function of the strain rate. Our developed model makes use of an empirical formula proposed first by Song and Xia (1994) for extensional viscosity that later applied by Feng (2002) for an electrospinning case.

We develop the polymeric fluid model for the rotating, slender jet by first deriving the governing equations and the boundary conditions for such fiber jet flow, and then determine the steady nonlinear solutions. We find some interesting results. In particular, we find as compared to Newtonian viscous fluid case, presence of extensional thinning of the polymeric fluid, which promotes stretching, can make the fiber jet radius and speed smaller

and higher, respectively, and the jet's stretching rate can be increased with polymeric jet relaxation time.

2.Governing system & modeling

Present rotating polymeric fiber jet flow is based on original governing equations for momentum and mass conservation (Chahhabra and Richardson 2008) in a rotating frame of reference that is attached and embedded on rotating spinneret (Figure 1) of forcespinning (FS) system. During FS process, produced fibers are curved due to rotational forces and can be collected at the end by a collector (figure 1) (Padron et al. 2013).

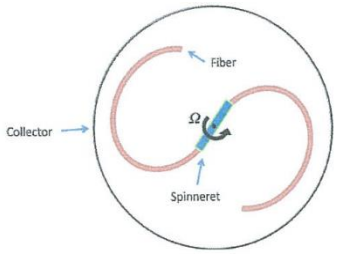


Figure 1.Forcespinning schematic. (The author acknowledges with thanks ASME as original publisher of this figure as well as figure 2 that granted him permission to include and print from "On 2D Forcespinning Modeling", by Simon Padron, Dumitru I. Caruntu & Karen Lozano. Paper Number IMECE2011-64823)

The governing equations of continuity and momentum equations in the rotating frame are

$$\nabla.\mathbf{u}=0, \quad (1a)$$

$$\partial\mathbf{u}/\partial t+ \mathbf{u}.\nabla\mathbf{u}=(-1/\rho)\nabla P +(1/\rho)\nabla.\mathbf{T}-\boldsymbol{\omega}\times(\boldsymbol{\omega}\times\mathbf{r})-2\boldsymbol{\omega}\times\mathbf{u}, \quad (1b)$$

where **u** is relative velocity vector of the fiber jet, P is pressure, **T** is stress tensor, ρ is density of the melt or solution, t is time variable, **ω** is angular velocity vector with magnitude Ω of the rotating spinneret whose orifice emits fiber jet from melt or solution in fluid container (Padron et al 2011, 2013), and **r** is a position vector of a point on fiber. We consider a Cartesian coordinate system (X, Y, Z) that is attached to the rotating spinneret and is referred to here as the rotating coordinated system. This coordinate system is fixed relative to the rotating spinneret.

We consider a two-dim model under fiber jet's arc length condition:

$$(\partial \mathbf{X}/\partial s)^2+(\partial \mathbf{Z}/\partial s)^2 =1, \qquad (1c)$$

where s is the arc length along the jet's centerline. It is assumed that components of position vector of a point on jet's centerline with respect to rotating Cartesian coordinate (X, Y, Z) system are c+**X**, **0** and **Z**, respectively

Equations (1a)-(1c) are subject to the boundary conditions at jet exit:

$$\mathbf{X}=\mathbf{Y}=\mathbf{Z}=\partial \mathbf{Y}/\partial s=\partial \mathbf{Z}/\partial s=0,\ \partial \mathbf{X}/\partial s=1,\ u=U,\ R=r_o \text{ at } s=0, \qquad (1d)$$

where U is centerline velocity of jet at the exit section and r_o is radius of the orifice at the jet exit section.

As observed in FS experiments (Padron et al. 2011; Padron et al. 2013), we consider rotating jet with curved centerline and set up rotating

system (Figure 2) with two coordinate systems, where one is fixed and other is attached to the rotating spinneret.

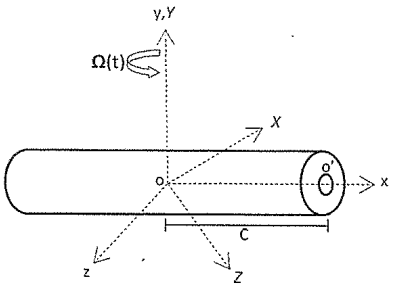


Figure 2.Two coordinate systems. (The author acknowledges with thanks ASME as original publisher of this figure as well as figure 1 that granted him permission to include and print from "On 2D Forcespinning Modeling", by Simon Padron, Dumitru I. Caruntu & Karen Lozano. Paper Number IMECE2011-64823)

In this figure, *c* represents the half-length of spinneret.

Our governing system (1a)-(1d) is studied by using empirical formula due to Song and Xia (1994) for the viscous contribution of the non-Newtonian polymeric fluid. So viscous stress term in momentum equation (1b) is modeled like

$$(1/\rho)\nabla.\mathbf{T} = (\mu/\rho)\nabla.(\eta\nabla\mathbf{u}), \qquad (2)$$

where μ is a reference (constant) dynamic viscosity and the expression for η is an empirical function of strain rate of polymeric fluid flow.

We non-dimensionalize system (1a)-(1d) and (2) in the already described local orthogonal coordinate system (s, n, ϕ) by using scaling U for velocity vector $\mathbf{u}=(u, v, w)$, ρU^2 for pressure, r_o for n and R, C for s and (X, Z), and C/U for t. Here C is half of length of the spinneret as a length scale in centerline direction of the jet (Padron et al. 2011). For simplicity of notation, the resulting non-dimensional system will be expressed in terms of the same original symbols. Non-dimensional form of the governing system contains some non-dimensional parameters, which are Rossby number $R_b=U/(\Omega C)$, Weber number $W_e=\rho U^2 r_o/\sigma$, Reynolds number $R_e=\rho UC/\mu$, Deborah number $D_e=\lambda U/C$ and a small aspect ratio parameter $\varepsilon=r_o/C$ ($\varepsilon<<1$), where λ is the relaxation time.

The non-dimensionalized system for FS that contains ε, is under the condition that fiber jet is a long and slender object, so that ε is a very small parameter ($\varepsilon<<1$). This suggests application of an asymptotic procedure in the limit of small ε for the governing system. Thus, we consider a slender jet where the velocity and pressure gradient are parallel to the center line at leading order. Following Parau et al. (2007) and Taghavi and Larson (2014a), we use a related expansions for dependent variables here

$$(u, v, w)= [u_0 (s, t)+\varepsilon n\, u_1(s, \phi, t)+\ldots, \varepsilon n\, v_1(s, \phi, t)+\ldots, \varepsilon n\, w_1(s, \phi, t)+\ldots], \quad (3a)$$

$$(P, R)=[P_0(s, t)+\varepsilon n P_1(s, \phi, t)+\ldots, R_0(s, t)+\varepsilon R_1(s, \phi, t)+\ldots], \quad (3b)$$

$$(X, Z)=[X_0(s, t)+\varepsilon X_1(s, t)+\ldots, Z_0(s, t)+\varepsilon Z_1(s, t)+\ldots]. \quad (3c)$$

Makes use of these expansions in the system, where the scaling factor ε is used to scale the variables. The governing system is then simplified and only the leading order terms in (1a)-(1d) are retained so that final system is only for u_0, R_0, X_0 and Z_0. Dropping the subscripts for simplicity of notations, the resulting simplified modeling FS system is given by

$$\partial u/\partial t + u(\partial u/\partial s) =[1/(W_e R^2)]\partial R/\partial s+(1/R_b^2)[(X+1)\partial X/\partial s+ Z \partial Z/\partial s]+(\eta/R_e)\{(3/R^2)[(\partial/\partial s)(R^2\partial u/\partial s)]- (\partial^2 u/\partial s^2)\}, \quad (4a)$$

$$\partial R/\partial t+ u\partial R/\partial s = -(R/2)\partial u/\partial s, \quad (4b)$$

$$(\partial X/\partial s)(\partial^2 X/\partial s^2)+(\partial Z/\partial s)(\partial^2 Z/\partial s^2)=0, \quad (4c)$$

$$(\partial Z/\partial s)(\partial^2 X/\partial t\partial s)-(\partial X/\partial s)(\partial^2 Z/\partial t\partial s)=\{u-[1/(W_e R u)]\}E -(2/R_b)+[1/(u R_b^2)][(X+1)(\partial Z/\partial s)-Z(\partial X/\partial s)]+(1/R_e)\{-2(\partial/\partial s)(\eta uE)+(\eta/3)(\partial/\partial s)(uE)-(\eta/2)(\partial u/\partial s)E\}, \quad (4d)$$

$$E\equiv[(\partial X/\partial s)(\partial^2 Z/\partial s^2)-(\partial Z/\partial s)(\partial^2 X/\partial s^2)], \quad (4e)$$

$$X=Z=\partial Z/\partial s=0,\ u=R=\partial X/\partial s=1 \text{ at } s=0, \quad (4f)$$

and empirical formula for η (Song and Xia 1994; Feng 2002) for extension thinning case is

$$\eta=[1+3 D_e^2(\partial u/\partial s)^2]^{(n-1)/2}, \quad (4g)$$

where n is a constant power law index.

As a result our stated scaling and due to the fact that to leading order terms in ε, the jet's velocity vector was found to be mainly along jet's centerline direction, the steady form of the resulting nonlinear system to the lowest order in ε is a system where dependent variables are all a function of the independent variable *s*, which is the arc length along the jet's centerline.

3.Solutions and results

We consider steady form of the solutions to system (4a)-(4f) for the present talk. We determine steady solutions to (4a)-(4f) both asymptotically for small arc length and numerically for arbitrary arc length.

Investigating the asymptotic form of steady solution of system (4a)-(4e) for small *s*, we find

$$u=1+a_1 s + a_2 s^2 + O(s^3), \tag{5a}$$

$$R=1-0.5a_1 s +(0.375\ a_1^2-0.5\ a_2)+O(s^3), \tag{5b}$$

$$X=s+ O(s^3), \tag{5c}$$

$$Z=c_1 s^2 + O(s^3), \tag{5d}$$

where the constants a_1 , a_2 and c_1 satisfy the following relations

$$a_1 [1+ 1/(2 W_e)]+(1/R_e)(3 a_1^2-4 a_2)[1+D_e^2 a_1^2]^{(n-1)/2}=(1/R_b^2), \tag{5e}$$

$$2(1-1/W_e)c_1+(c_1a_1/R_e)\{8(1-n) a_2 D_e^2[1+D_e^2 a_1^2]^{(n-3)/2}-(13/3)[1+D_e^2 a_1^2]^{(n-1)/2}\}=(2/R_b). \tag{5f}$$

These solutions agree with the corresponding ones for inviscid case obtained by Decent et al. (2002) in the limit of $R_e = \infty$. These asymptotic results (5a)-(5f) are also useful for our numerical solutions of full steady solutions of (4a)-(4f), which are described below, since such solutions are based on using an initial value problem.

We solved steady nonlinear system (4a)-(4f) numerically by treating it as an initial value problem with independent variable s using an efficient Runge-Kutta scheme of fourth order (Ascher et al., 1995).

Since the viscous stress terms contain second derivative for u and third derivatives for both X and Z, we make use of asymptotic solutions (5a)-(5f) at $s=0$ which require knowing values of constants a_1 and c_1 as given by (5e)-(5f). However, these two equations contain additional unknown constant a_2. We tried a given value of a_2 and calculate iteratively a_1 from (5e) and then used the values of a_1 and a_2 in (5f) to determine the value of c_1. We then carried out numerical solution of IVP. We did such calculations for several prescribed values of a_2 and found that numerical solution for the rate of increase of $\partial u/\partial s$ at $s=0$ is very small of order 10^{-3} or less and is rather insensitive to the value of a_2 that is chosen in (5e)-(5f) to evaluate a_1 and c_1. We, thus, carried out our actual numerical calculation of IVP by assuming $a_2 = 0$. We generated data for the jet centerline speed, jet radius, jet trajectory,

strain rate and stretching rate for different values of the parameters R_e, D_e, R_b, W_e and n.

We found that for present FS problem of a polymeric fluid flow case, jet speed increases and jet radius decreases with decreasing R_b or with increasing W_e. These results are reasonable since smaller Rossby number implies larger rotational forces which can enhance polymeric fiber jet speed and can make fiber jet thinner as observed experimentally (Padron et al., 2013), and the result that the speed of the polymeric fiber jet decreases and its radius increases as the Weber number decreases, is due to the force resisting the thinning of the fiber.

We also generate data for jet speed versus arc length for W_e =1.5, R_b =0.8, D_e =n=1 and two different values 0.1 and 1.0 of the Reynolds number. We find from our data stabilizing effect of viscosity (for lower values of Reynolds number) that is enhanced with increasing the arc length.

Figures 3-5 present typical results about the effects of extension thinning of the polymeric fluid flow on the jet speed, jet radius and jet trajectory. Figure 3 presents the centerline velocity versus arc length for R_b =0.8, We=1.5 and different values of Deborah number and the index n. It can be seen from this figure that jet speed increases with the

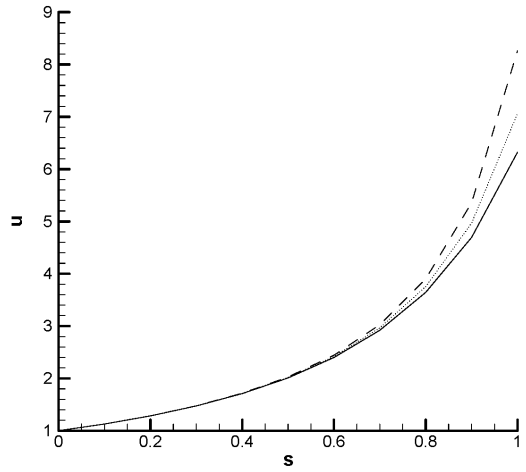


Figure 3.*u* versus *s* for R_b =0.8, W_e =1.5 and for D_e=0.58, *n*=1(solid line), D_e =5.8, *n*=0.8(dotted line) and D_e =57.7, *n*=0.8(dashed line).

arc length and also with increasing the effect of the polymeric extension thinning. This result suggests that the presence of polymeric fluid flow and significant extension thinning can contribute to the speed up the fiber jet.

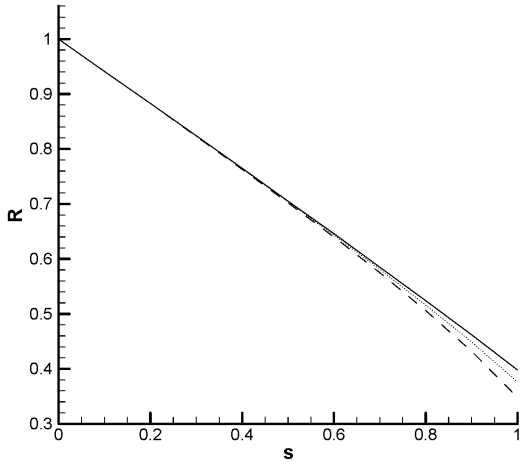


Figure 4.The same as in figure 3 but for jet radius *R*

Figure 4 presents jet radius versus arc length for R_b =0.8, W_e =1.5 and different values of the Deborah number and the index n. It can be seen from this figure that jet radius decreases with increasing the arc length and the extensional thinning effect, which again indicate similar roles played by the extensional polymeric fluid flow.

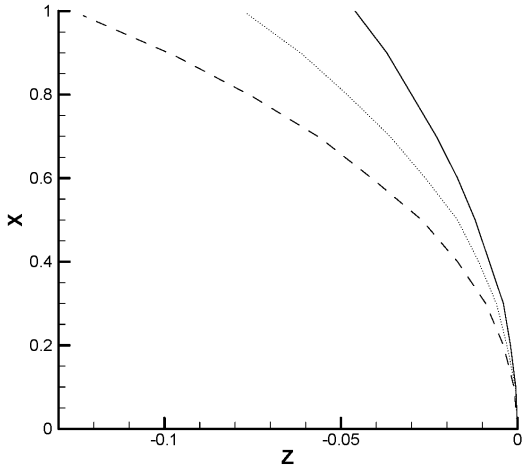


Figure 5.The same as in figure 3 but for jet trajectory

Figure 5 presents jet trajectory in (X, Z)-plane for R_b =0.8, W_e =1.5 and different values of the Deborah number and the index n. As can be seen from this figure, the effect of the extensional thinning of the polymeric fluid flow is to decrease locally the radius of curvature of the trajectory.

Figures 6-7 present strain rate ($\partial u/\partial s$) and stretching rate ($\partial R/\partial s$), respectively, versus arc length for W_e =1.5, R_b =0.8, R_e =0.1, and for different values of Deborah number and index n. It can be seen from figure 6 that strain rate of fiber

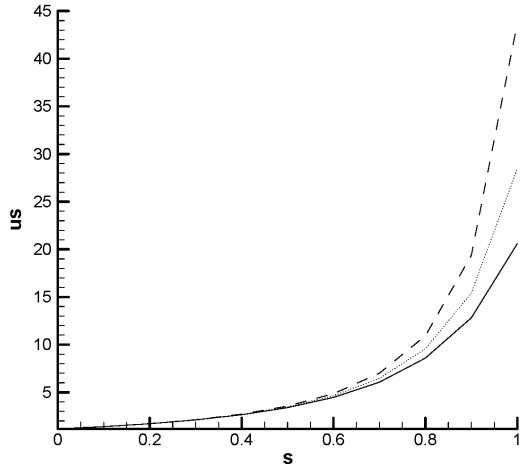


Figure 6.Strain rate versus arc length for W_e=1.5, R_b=0.8, R_e=0.1 and for different values of the Deborah number and the index n: D_e =0.58, n=1 (solid line); D_e =5.8, n=0.8 (dotted line); D_e =57.7, n=0.8 (dashed line).

jet increases with arc length and extensional rheology of the polymeric flow, and such extensional thinning increases at a higher rate as arc length increases. Figure 7, which presents the stretching rate versus the arc length shows similar behavior to that of the strain rate, where the rate of stretching increases with the arc length as well as with extensional thinning of the fiber jet.

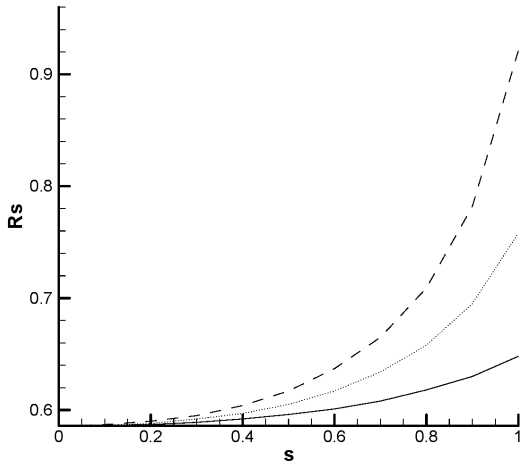


Figure 8.The same as in figure 7 but for stretching rate.

More Recent Work:

Recently we have investigated aerodynamic drag force on the fiber jet production (Riahi, 2018) as well as joint work with inclusion of experimental studies (Riahi, Lozano, Cremar & Fuentes, 2018) with general agreement of the present modeling results and those of experiments.

5.Concluding remarks

We developed a non-Newtonian viscosity model for rotating polymeric fiber jets during forcespinning that focuses on extensional thinning aspects of the polymeric fluid flow. We considered the nonlinear steady form of the governing system for rotating fiber jet and determined its solutions asymptotically as well as numerically. We found that the jet speed,

jet radius, strain rate and stretching increase with increasing extensional thinning effect, rotational effect or the distance from orifice. In addition, the jet radius and jet speed increases and decreases, respectively, with increasing either viscosity or surface tension effects.

Padron et al. (2013) and Riahi et al. (2018) used high speed photography to provide some understanding on the mechanisms involved for the production of fiber jets through FS. They also determined the effects of controllable parameters such as angular velocity of the rotating spinneret and viscosity effect of the polymeric solution, which was a weight percentage of PEO (Polyethylene oxide) concentration in water, on fiber jet trajectory, jet speed and jet diameter. These experimental results are qualitatively in agreement with present theoretical and numerical results.

The present results for the polymeric fiber jet properties can be useful for ways that can be searched to improve nano fiber jet production of high yield as well as to stimulate further experimental studies to provide quantitative results on effective polymeric jets that affect final production of actual nano fibers. Further extensions of the present work to include additional polymeric effect such as viscoelastic effects for the fiber jet production by FS process as well as stability of the steady solutions will be investigated by present author in near future.